

Submitted to the Astrophysical Journal

Large-Scale Intrinsic Alignment of Galaxy Images

Tereasa G. Brainerd, Ingolfur Agustsson, Chad A. Madsen

*Boston University, Institute for Astrophysical Research, 725 Commonwealth Ave., Boston,
MA 02215*

brainerd@bu.edu, ingolfur@bu.edu, cmadsen@bu.edu

and

Jeffrey A. Edmonds

*Boston University, Dept. of Religious and Theological Studies, 145 Bay State Road,
Boston, MA 02215*

jedmonds@bu.edu

ABSTRACT

We compute the two-point image correlation function for bright galaxies in the seventh data release of the Sloan Digital Sky Survey (SDSS) over angular scales $0.01' \leq \theta \leq 120'$ and projected separations $0.01 \text{ Mpc} \leq r_p \leq 10 \text{ Mpc}$. We restrict our analysis to SDSS galaxies with accurate spectroscopic redshifts, and we find strong evidence for intrinsic alignment of the galaxy images. On scales greater than $r_p \sim 40 \text{ kpc}$, the intrinsic alignment of the SDSS galaxy images compares well with the intrinsic alignment of galaxy images in a Λ CDM universe, provided we impose Gaussian-random errors on the position angles of the theoretical galaxies with a dispersion of $\sigma_\phi = 25^\circ$. Without the inclusion of these errors, the amplitude of the two-point image correlation function for the theoretical galaxies is a factor of ~ 2 higher than it is for the SDSS galaxies. We interpret this as a combination of modest position angle errors for the SDSS galaxies, as well as a need for modest misalignment of mass and light in the theoretical galaxies. The intrinsic alignment of the SDSS galaxies shows no dependence on the specific star formation rates of the galaxies and, at most, a very weak dependence on the colors and stellar masses of the galaxies. At the $\sim 3\sigma$ level, however, we find an indication that the images of the most luminous SDSS galaxies are more strongly aligned with each other than are the images of the least luminous SDSS galaxies.

Subject headings: cosmology: observations — galaxies: formation — galaxies: halos — large-scale structure of the universe — methods: statistical

1. Introduction

The intrinsic alignment of galaxy images is of great interest for several reasons. First, observations of intrinsic alignments of galaxies over large scales constitute a test of galaxy formation models. Numerous numerical and analytical studies have shown that galaxies should be intrinsically aligned with each other over large scales in the universe (e.g., Heavens & Peacock 1988; Heavens et al. 2000; Catelan et al. 2001; Crittenden et al. 2001, 2002; Croft & Metzler 2001; Lee & Pen 2001; Jing 2002; Mackey et al. 2002; Porciani et al. 2002; Aubert et al. 2004; Heymans et al. 2004, 2006; Hirata & Seljak 2004; Lee et al. 2008; Okumura et al. 2009; Schneider & Bridle 2009). Observations of intrinsic alignments of galaxies can, therefore, be used as consistency checks on theories of galaxy formation. Further, they can be used to place constraints on the degree to which the images of luminous galaxies are aligned with their dark matter halos.

In addition, intrinsic alignments of galaxies could be an important contributor of “false signal” in studies that seek to measure weak gravitational lensing by large-scale structure (a.k.a. cosmic shear). To a first approximation, weak lensing by large-scale structure tends to make galaxies that are nearby to each other on the sky “point” in the same direction (see, e.g., Fig. 1 of Blandford et al. 1991). Cosmic shear requires substantial depths (i.e., moderate to large source redshifts) in order to be detectable. Even still, in a deep, weak lensing data set care must be taken to account for any contribution of intrinsic galaxy alignments to the observed signal and, hence, in the subsequent quantification of cosmic shear. In principle this can be done either by eliminating galaxies that are nearby to one another (in both position on the sky and redshift) or by modelling the expected contributions of intrinsic alignments to the measured signal (see, e.g., Heymans & Heavens 2003; King & Schneider 2003; Heymans et al. 2004; Takada & White 2004; Bridle & King 2007; Joachimi & Schneider 2008; Kitching et al. 2008; Zhang 2008). Therefore, in order to obtain the best constraints on weak lensing by large-scale structure, it is important to know the degree to which galaxies are intrinsically aligned, including the scales over which the intrinsic alignment manifests in our universe.

The first tentative detections of intrinsic alignments of galaxy images (Brown et al. 2003; Heymans et al. 2004) did not include spectroscopic redshift information that could be used to identify galaxies that are physically nearby to one another. More recent detections (Agustsson & Brainerd 2006a; Lee & Pen 2007; Okumura et al. 2009) have used both photometric and spectroscopic information from the Sloan Digital Sky Survey (SDSS; Fukugita

et al. 1996; York et al. 2000; Hogg et al. 2001; Smith et al. 2002; Strauss et al. 2002; Ivezić et al. 2004)) in order to restrict the analysis to galaxies that are nearby to one another and, hence, to optimise the probability of detecting the signature of intrinsic alignment.

Agustsson & Brainerd (2006a; hereafter AB06a) used the fourth data release (DR4) of the SDSS to investigate the degree to which the images of satellite galaxies were aligned with their “host” galaxies. The sample consisted of 3180 host galaxies that were relatively isolated in space (more isolated than the Milky Way or M31) and 4289 satellite galaxies. For projected separations less than $r_p \sim 30$ kpc, AB06a found a tendency for the images of the satellite galaxies to be aligned in the same direction as the images of their hosts. Lee & Penn (2007; hereafter LP07) used 434,849 galaxies from the sixth data release of the SDSS to investigate differences between the intrinsic alignments of red and blue galaxies as a function of three-dimensional separation. LP07 restricted their analysis to galaxies that had spectroscopic redshifts and $M_r \leq -19.2$. Over separations $r \leq 5h^{-1}$ Mpc, LP07 found a tendency for the images of the red galaxies to be aligned. LP07 also found a tendency for the images of the blue galaxies to be aligned, but only over separations $r \leq 3h^{-1}$ Mpc.

Perhaps the most convincing detection of intrinsic alignment of galaxy images to date is the work of Okumura et al. (2009; hereafter OJL). OJL restricted their analysis to the 83,773 Luminous Red Galaxies (LRGs) in the SDSS and computed the two-point image correlation function over three dimensional separations $r \sim 1h^{-1}$ Mpc to $r \sim 130h^{-1}$ Mpc. OJL found a strong detection of the two-point image correlation function for the images of the SDSS LRGs over these scales. However, when OJL compared their results to a prediction of the intrinsic alignment expected for elliptical galaxies in a Λ CDM universe, they found that the predicted two-point image correlation function had an amplitude that was a factor ~ 4 larger than they observed for the SDSS LRGs. In order to compute the theoretical image correlations, OJL made the common assumption that luminous elliptical galaxies share the shapes of their dark matter halos (i.e., perfect alignment of mass and light). OJL then interpreted the discrepancy between the observed and predicted two-point image correlation functions as evidence for a substantial misalignment of mass and light in elliptical galaxies ($\sigma_\theta = 35.4_{-3.3}^{+4.0}$ degrees).

Given the observed anisotropic distribution of satellite galaxies around relatively isolated host galaxies (e.g., Brainerd 2005; Agustsson & Brainerd 2007; Azzaro et al. 2007; Bailin et al. 2008; Siverd et al. 2009), as well as observations of weak gravitational lensing by the flattened halos of field galaxies (e.g., Hoekstra et al. 2004; Mandelbaum et al. 2006; Parker et al. 2007), it would be surprising if the images of elliptical galaxies were as badly misaligned from their halos as is suggested by OJL. In the case of satellite galaxies, the satellites of relatively isolated red host galaxies are located preferentially nearby the major axes of their

hosts, both in the SDSS and in Λ CDM universes (e.g., Agustsson & Brainerd 2007). If the images of the red Λ CDM host galaxies are misaligned with respect to their dark matter halos by a very large amount, the anisotropy in the locations of the satellites is reduced well below the level that is detected for the satellites of red SDSS host galaxies.

In the case of weak lensing by flattened halos, one essentially has to assume a reasonable alignment of mass and light in the lenses in order to search for an anisotropy in the weak lensing signal. That is, if mass and light are badly misaligned for the lens galaxies, one will measure an isotropic lensing signal on average since the only symmetry axes that one can use for the measurement are the symmetry axes of the lensing galaxies themselves. Although detection of anisotropic galaxy–galaxy lensing is difficult, it has been tentatively observed for red lens galaxies (e.g., Mandelbaum et al. 2006; Parker et al. 2007). This is an indication, then, that mass and light are at least reasonably well–aligned in the case of red field galaxies. Similarly, in their study of strong gravitational lenses, Keeton et al. (1998) found that the mass and light of early–type galaxies was aligned to within $\sim 10^\circ$.

Here we investigate the intrinsic alignment of galaxy images in the seventh data release (DR7; Abazajian et al. 2009) of the SDSS. We restrict our analysis to galaxies that are intrinsically rather bright, have well-determined spectroscopic redshifts, and which are located at sufficiently low redshifts that their image shape parameters should be determined reasonably well. The paper is organized as follows. In §2 we describe the subset of the SDSS DR7 galaxies that we use for our study, we compute the intrinsic alignment of the SDSS galaxies using a two–point image correlation function, and we subject the data to a number of null tests in order to check for the presence of systematics. In §3 we compare the intrinsic alignment of the images of SDSS galaxies to the expectations for galaxies in a Λ CDM universe. In §4 we investigate the degree to which the intrinsic alignment signal depends upon various physical parameters: color, luminosity, stellar mass, and star formation rate. Lastly, in §5 we present a discussion of our results and our conclusions. Throughout we adopt cosmological parameters $H_0 = 73 \text{ km sec}^{-1} \text{ Mpc}^{-1}$, $\Omega_{m0} = 0.25$, and $\Omega_{\Lambda0} = 0.75$.

2. Intrinsic Alignments of SDSS Galaxy Images

For our observational dataset we select all SDSS DR7 galaxies with Petrosian apparent magnitudes in the range $13.0 \leq r \leq 17.77$, absolute magnitudes in the range $-23.0 \leq M_r + 5 \log_{10} h \leq -19.0$, and spectroscopic redshifts with $z_{\text{conf}} > 0.9$. There are a total of 530,397 galaxies in the SDSS DR7 that satisfy these criteria. The median redshift of the sample is $z_{\text{med}} = 0.09$, and the maximum redshift is $z_{\text{max}} = 0.20$. In analogy to weak lensing

analyses, we define a complex image shape parameter for each of the galaxies as

$$\vec{\chi} \equiv \epsilon e^{2i\phi}, \quad (1)$$

where $\epsilon = (a - b)/(a + b)$, a is the semi-major axis of the galaxy, b is the semi-minor axis of the galaxy, and ϕ is its position angle. Throughout we use shape parameters that have been computed using the SDSS r -band photometry.

Also in analogy with the statistical measures that are commonly used to quantify weak lensing by large-scale structure, we define a two-point correlation function for galaxy images as

$$C_{\chi\chi}(\theta) \equiv \langle \vec{\chi}_1 \cdot \vec{\chi}_2^* \rangle_\theta \quad (2)$$

which measures the degree to which the image of galaxy 1 is aligned with the image of galaxy 2, averaged over angular scales $\theta \pm d\theta/2$ (e.g., Blandford et al. 1991). The function $C_{\chi\chi}(\theta)$ is positive if the major axes of the galaxies are aligned with one another on average, it is zero if the major axes of the galaxies are oriented randomly on average, and it is negative if the major axes are oriented at right angles to one another on average.

Since we expect that galaxies will be not be intrinsically aligned over extremely large physical scales in the universe, we restrict our analysis to pairs of galaxies that are relatively close to each other in velocity space. That is, pairs of galaxies that are separated by many hundreds of megaparsecs along the line of sight are unlikely to be intrinsically aligned, while pairs of galaxies that are separated by a few tens of megaparsecs along the line of sight should be intrinsically aligned to at least some degree. This in mind, we compute $C_{\chi\chi}(\theta)$ for pairs of galaxies with line of sight velocity differences $|dv| \leq 5000 \text{ km sec}^{-1}$. Fig. 1 shows the result of this computation for SDSS DR7 galaxies that are separated by angles $0.01' \leq \theta \leq 120'$ on the sky. The function has been computed using angular bins that are equally-spaced in the logarithm, and the error bars show the standard deviation in the mean of $C_{\chi\chi}(\theta)$.

It is clear from Fig. 1 that the images of the SDSS galaxies have a small but detectable tendency to be aligned with each other over large angular scales on the sky. To investigate whether the result in Fig. 1 is genuine (and, therefore, indicative of intrinsic alignment of the galaxies) or whether it can be attributed to a systematic, we perform a number of null tests. First, we compute $C_{\chi\chi}(\theta)$ exactly as we did in Fig. 1, but we restrict the analysis to pairs of galaxies that are separated by large amounts in velocity space ($5000 \text{ km sec}^{-1} < |dv| \leq 10,000 \text{ km sec}^{-1}$). Second, we randomize the declinations of the galaxies (i.e., swapping the declinations amongst the galaxies so that galaxy i is assigned the declination of galaxy j) while maintaining the observed right ascensions and redshifts of the galaxies. Third, we perform a classic weak lensing null test in which we rotate the observed position angles by 45° . Lastly, we randomize the position angles of the galaxies by swapping the

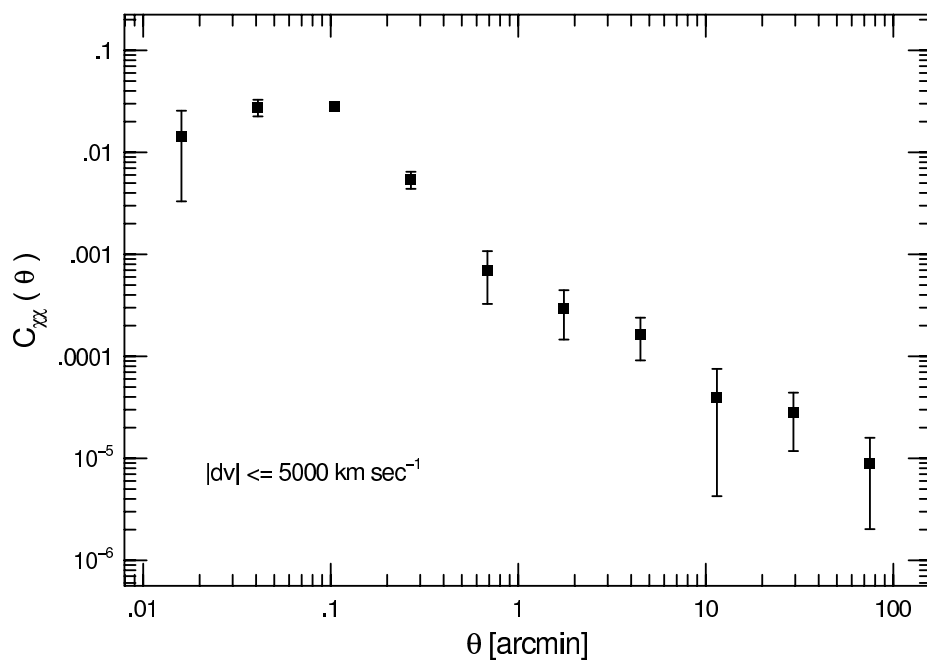


Fig. 1.— Two-point correlation function of image shapes for SDSS galaxies computed using pairs of galaxies with angular separations $0.01' \leq \theta \leq 120'$. Pairs of galaxies are restricted to line of sight velocity differences $|dv| \leq 5000 \text{ km sec}^{-1}$. Error bars show the standard deviation in the mean of $C_{xx}(\theta)$.

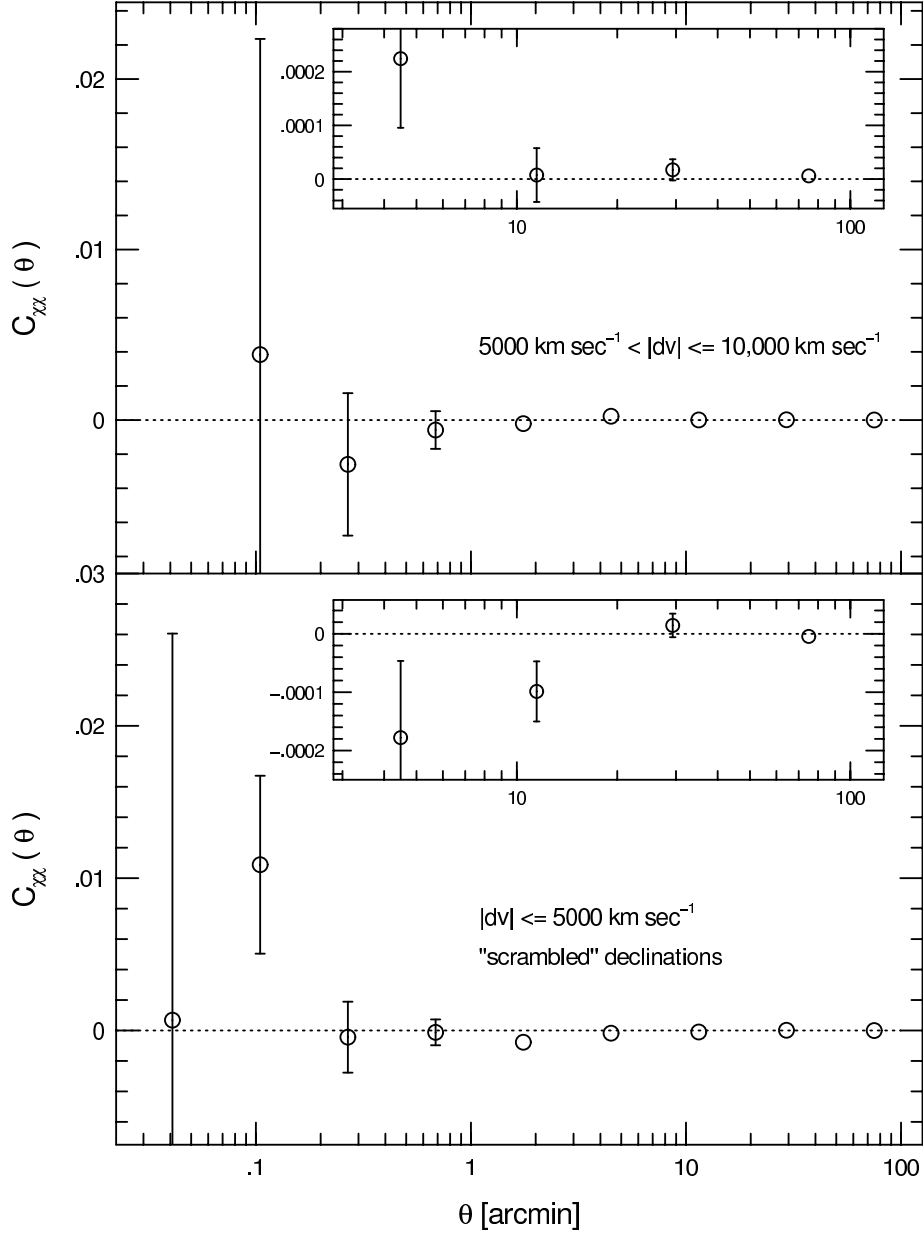


Fig. 2.— Null tests using the two-point correlation function of image shapes for SDSS galaxies. Top panel: $C_{xx}(\theta)$ computed as in Fig. 1, but here the pairs of galaxies are separated by line of sight velocity differences of $5000 \text{ km sec}^{-1} < |dv| \leq 10,000 \text{ km sec}^{-1}$. Bottom panel: $C_{xx}(\theta)$ computed as in Fig. 1, but here the declinations of the galaxies have been scrambled. Error bars are omitted in the case that the error bar is smaller than the data point. Insets show $C_{xx}(\theta)$ for the last 4 bins on an expanded scale. Note that in the top panel there are no pairs of galaxies that fall into the first two angle bins of Fig. 1. In the bottom panel, there are no pairs of galaxies that fall into the first angle bin of Fig. 1.

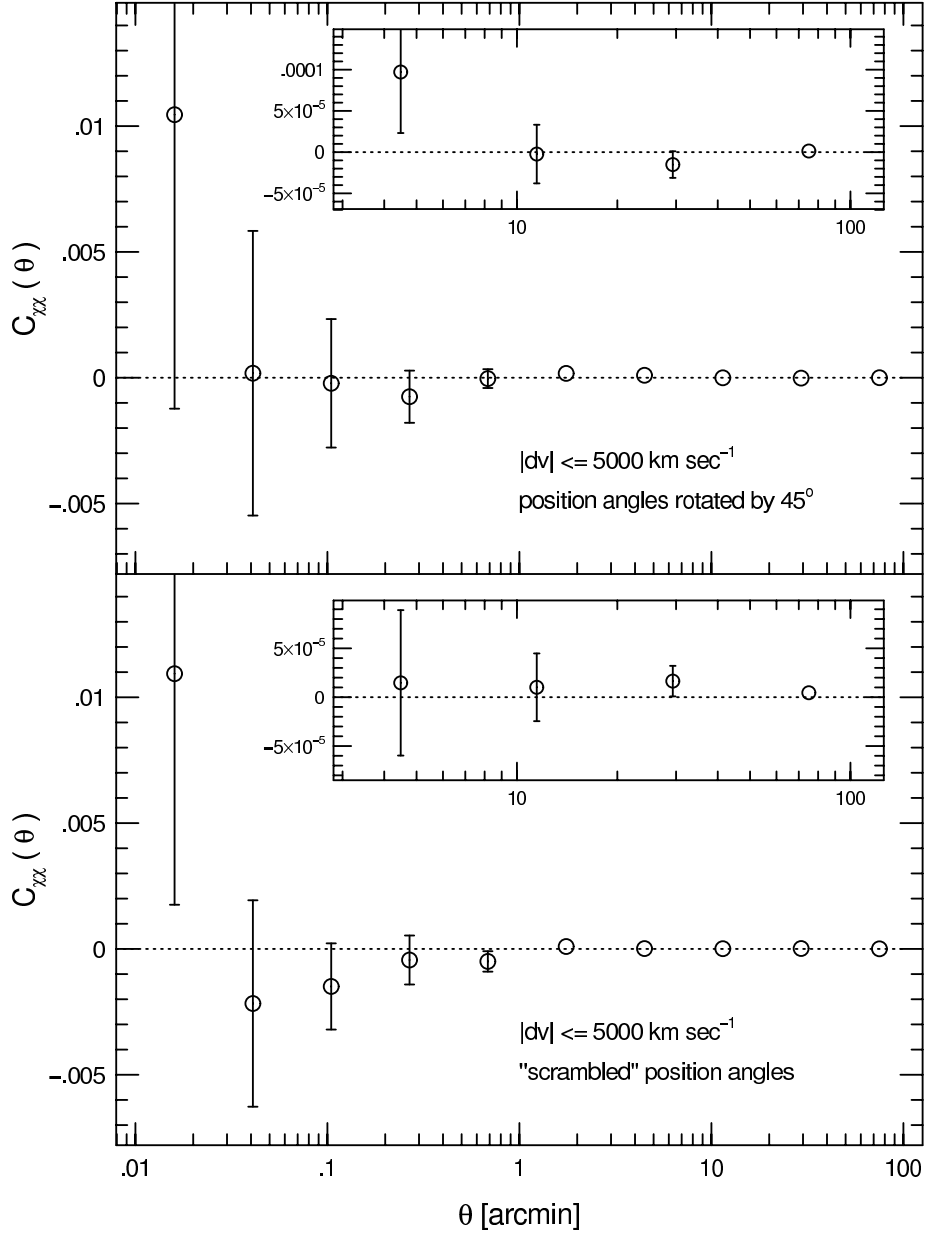


Fig. 3.— Null tests using the two-point correlation function of image shapes for SDSS galaxies. Top panel: $C_{xx}(\theta)$ computed as in Fig. 1, but here the position angles of the galaxies have been rotated by 45° . Bottom panel: $C_{xx}(\theta)$ computed as in Fig. 1, but here the position angles of the galaxies has been scrambled. Error bars are omitted in the case that the error bar is smaller than the data point. Insets show $C_{xx}(\theta)$ for the last 4 bins on an expanded scale.

observed position angles amongst the galaxies (i.e., the position angle of galaxy i is assigned to galaxy j). In the last three null tests we restrict the pairs of galaxies to be separated by $|dv| \leq 5000 \text{ km sec}^{-1}$, as we did for the calculation in Fig. 1. The function $C_{\chi\chi}(\theta)$ ought to vanish for all of the null tests if the signal shown in Fig. 1 is genuine and not due to an artifact in the data.

The results of the first two null tests are shown in Fig. 2 and the results of the second two null tests are shown in Fig. 3. In all cases, $C_{\chi\chi}(\theta)$ for the null tests is consistent with the images of the galaxies being uncorrelated. Therefore, the alignment exhibited in Fig. 1 is unlikely to be caused by a systematic.

3. Comparison to Intrinsic Alignment of Galaxy Images in a Λ CDM Universe

We now investigate whether the apparent intrinsic alignment of the SDSS galaxies in the previous section is consistent with the expectations for bright galaxies in a Λ CDM universe. To do this we make use of the Millennium Run Simulation (MRS; Springel et al. 2005) and the corresponding MRS mock galaxy redshift catalog that was constructed by Blaizot et al. (2005) using the Mock Map Facility (MoMaF). The MRS is a large simulation of the growth of structure in a Λ CDM universe that has both high spatial resolution and high mass resolution (softening length of $5h^{-1}$ kpc and particle mass $m_p = 8.6 \times 10^8 h^{-1} M_\odot$). Although the MRS particle files are not publicly-available due to their enormous size, information about the dark matter halos, subhalos, and the luminous galaxies (as determined from semi-analytic galaxy formation codes) is publicly-available¹. The mock redshift catalog for the MRS galaxies is also publicly-available².

Stellar masses, star formation rates, bulge-to-disk ratios, luminosities, colors, and dark matter halo masses are all publicly-available for the MRS galaxies. Importantly for our work, however, is that there is no information on the observed *shapes* of the luminous galaxies in the MRS. In order to compare the intrinsic alignment of the SDSS galaxies to the expectations of a Λ CDM universe, we therefore need to choose a method by which to *assign* shapes to the MRS galaxies. To do this, we use the B-band bulge-to-disk ratios ($\Delta M(B) = M(B)_{\text{bulge}} - M(B)_{\text{total}}$) from the semi-analytic galaxy formation model of De Lucia et al. (2006) to classify the MRS galaxies into three broad categories: ellipticals, lenticulars, and spirals. Following De Lucia et al. (2006), we consider MRS galaxies with $\Delta M(B) < 0.4$ to be ellipticals

¹<http://www.mpa-garching.mpg.de/millennium/>

²<http://galics.iap.fr>

and those with $0.4 \leq \Delta M(B) \leq 1.56$ to be lenticulars. In addition, we assume that all MRS galaxies with $\Delta M(B) > 1.56$ that will be used in our analysis are spiral galaxies. In principle galaxies with $\Delta M(B) > 1.56$ could be irregulars, but given that we are restricting our analysis to galaxies with rather bright luminosities ($-23.0 \leq M_r + 5 \log_{10} h \leq -19.0$; see §2), it is unlikely that any MRS galaxy with $\Delta M(B) > 1.56$ that meets our minimum luminosity criterion would be an irregular.

In order to assign observed shapes to the MRS galaxies (i.e., observed position angles and ellipticities), we adopt a very simple prescription. We assume that ellipticals share the same shapes as their dark matter halos, and we assume that all disk galaxies (i.e., the spirals and lenticulars) are circular disks whose angular momentum vectors are perfectly aligned with the net angular momentum vectors of their dark matter halos. The angular momentum vectors of the dark matter halos that we require for the disk galaxies are publicly-available; however, the moments of inertia of the halos are not publicly-available. Therefore, in order to assign shapes to the elliptical galaxies we need to adopt a proxy for the mass distribution within the halos. Previous work using the Λ CDM GIF simulation has shown that small satellite galaxies trace the shapes of the halos that surround the large, primary galaxies about which the satellites are orbiting (Agustsson & Brainerd 2006b). Therefore, to determine the shape of a halo surrounding an elliptical MRS galaxy, we use the locations of its satellites as a proxy for the mass distribution of the halo. We restrict our analysis to elliptical galaxies that have at least 4 satellites within the virial radius, and using these we compute a 3-dimensional ellipsoid that defines the shape of the galaxy.

Of order 5% of the MRS galaxies that fall within the luminosity range that we have adopted have been stripped of all of their dark matter due to numerical effects. These are referred to as “type 2” galaxies in the De Lucia & Blaizot (2007) semi-analytic model for the MRS galaxies, and all are satellite galaxies that are orbiting within the dark matter halo of a larger galaxy. Since there is no dark matter substructure around the type 2 galaxies, we cannot assign observed shapes to them and we therefore do not use them in our analysis. The loss of these galaxies will restrict our ability to measure the intrinsic alignments on small physical scales (i.e., scales much less than the virial radii of the halos of large galaxies) since these galaxies contribute a great deal to the pair counts at small separations. On larger scales, however, the pair counts are heavily dominated by the galaxies for which we can measure the shapes, and the loss of the type 2 galaxies from the analysis will have no affect on the results. In total, there are 3.1×10^6 MRS galaxies that fall within our adopted luminosity range and for which we can assign shapes.

To obtain the observed position angles and ellipticities of the MRS galaxies, we project the 3-dimensional shapes of the galaxies (i.e., ellipsoids or circular disks) onto the sky using

the galaxy locations from the mock redshift survey of Blaizot et al. (2005). We then compute the complex image shape parameter, $\vec{\chi}$, for each MRS galaxy in exactly the same way as it was computed for the SDSS galaxies.

To compare the degree of alignment of the galaxy images in the SDSS DR7 and in the MRS, we compute the two–point image correlation function as a function of projected separation on the sky, $C_{\chi\chi}(r_p)$. We expect this to provide a more reasonable comparison than the two–point image correlation function computed as a function of angular separation, $C_{\chi\chi}(\theta)$. This is because, although the redshift distributions of the SDSS galaxies and the MRS mock redshift survey galaxies are very similar, they are not identical. This will affect the number of pairs found a given angular separation, θ , somewhat more than it will affect the number of pairs found to be separated by a given projected separation, r_p . This is due to the fact that when we calculate $C_{\chi\chi}(\theta)$ we do not account for the specific value of the line of sight velocity difference between the two galaxies (i.e., we simply accept all pairs of galaxies with $|dv| \leq 5000 \text{ km sec}^{-1}$). In the case of $C_{\chi\chi}(r_p)$ we make use of the specific value of the velocity difference in addition to the angular separation.

In both the SDSS and MRS we define the projected separation between a pair of galaxies to be

$$r_p \equiv \frac{\theta}{2} (D_{A1} + D_{A2}) \quad (3)$$

where θ is the angular separation between the galaxies (in radians), D_{A1} is the angular diameter distance to galaxy 1, and D_{A2} is the angular diameter distance to galaxy 2. We compute the angular diameter distances for the SDSS and MRS galaxies in the standard way using their observed redshifts and our adopted cosmological parameters. The resulting two–point correlation functions are shown in Fig. 4.

As in §2, we restrict our analysis in Fig. 4 to galaxies with absolute magnitudes in the range $-23.0 \leq M_r + 5 \log_{10} h \leq -19.0$. We then compute $C_{\chi\chi}(r_p)$ for galaxy pairs separated by $0.01 \text{ Mpc} \leq r_p \leq 10 \text{ Mpc}$. From Fig. 4, we see that the degree of intrinsic alignment of the galaxy images in the SDSS is comparable to that in a Λ CDM universe. In the first bin, $C_{\chi\chi}(r_p)$ for the MRS galaxies sits quite low compared to $C_{\chi\chi}(r_p)$ for the SDSS galaxies. The discrepancy is most likely due to the fact that on such small scales (i.e., $r_p \sim 15 \text{ kpc}$) we simply do not have the ability to measure $C_{\chi\chi}(r_p)$ accurately for the MRS galaxies. Roughly 80% of the galaxy pairs in the MRS that ought to go into the calculation of $C_{\chi\chi}(r_p)$ in the first bin include at least one “type 2” galaxy (i.e., a galaxy for which we cannot assign a shape due to the fact that it has been stripped of all dark matter). That is, on the smallest physical scales the two–point correlation function of image shapes is dominated by the degree to which large galaxies and their satellites are aligned with each other, and we simply do not have the ability to measure this well for the MRS galaxies. To further emphasize that

the primary contributors to intrinsic alignments on small scales are the images of satellites and the galaxies which they orbit, we also show in Fig. 4 (stars) the small-scale intrinsic alignment found by AB06a for the images of relatively isolated SDSS host galaxies and their satellites. The agreement between the results of AB06a and our present analysis of SDSS DR7 galaxies is quite good, demonstrating that intrinsic alignment of galaxy images at the smallest projected radii is largely attributable to galaxies that are physically quite close together in space.

Fig. 4 shows that on scales larger than $r_p \sim 40$ kpc, the intrinsic alignment of the MRS galaxy images is somewhat stronger than that of the SDSS galaxy images. Overall, the amplitude differs by a factor of order 2 on these scales. In their analysis of the intrinsic alignments of galaxies, OJL also found that the images of elliptical galaxies in a Λ CDM universe showed a greater degree of intrinsic alignment than did the images of the SDSS luminous red galaxy (LRG) sample. Like us, OJL assumed that elliptical galaxies shared the shapes of their halos and they found that the two-point correlation function of image shapes was a factor of order 4 larger for the Λ CDM ellipticals than it was for the SDSS LRGs. To explain this discrepancy, OJL argue that the Λ CDM galaxy images must be misaligned with respect to their halos, and that the misalignment is quite large indeed ($\sigma_\theta = 35.4_{-3.3}^{+4.0}$ degrees).

We now consider the degree to which the position angles of the MRS galaxy images must differ from the values used in Fig. 4 in order to yield a two-point image correlation function that matches that of the SDSS galaxies. To do this, we assign Gaussian-random errors to the position angles of the MRS galaxies and we recompute $C_{\chi\chi}(r_p)$ using these “corrupted” position angles. Shown in Fig. 5 is the result for $C_{\chi\chi}(r_p)$ in which Gaussian-random errors with zero mean and dispersion $\sigma_\phi = 25^\circ$ have been assigned to the position angles of the MRS galaxies. From this figure, then, it is clear that on scales larger than $r_p \sim 40$ kpc, there is good agreement between the intrinsic alignments of the SDSS and MRS galaxies if the typical error in the position angle is of order 25° . This is substantially smaller than the galaxy-halo misalignment required by OJL, but is consistent with the galaxy-halo misalignment required by Faltenbacher et al. (2009) in their study of the alignments of bright, red galaxies with local large-scale structure. In addition, if we increase the dispersion for the position angles of the MRS galaxies to $\sigma_\phi = 35^\circ$, $C_{\chi\chi}(r_p)$ for the MRS galaxies becomes consistent with zero (i.e., we can no longer detect intrinsic alignments using our theoretical galaxy images if the error in the position angle has such a large dispersion).

We also note that the shape parameters of the images of the SDSS galaxies cannot be measured with infinite accuracy; i.e., there is some noise in the determination of $\vec{\chi}$ for all SDSS galaxies. The function $C_{\chi\chi}(r_p)$ is not particularly sensitive to errors in the ellipticities

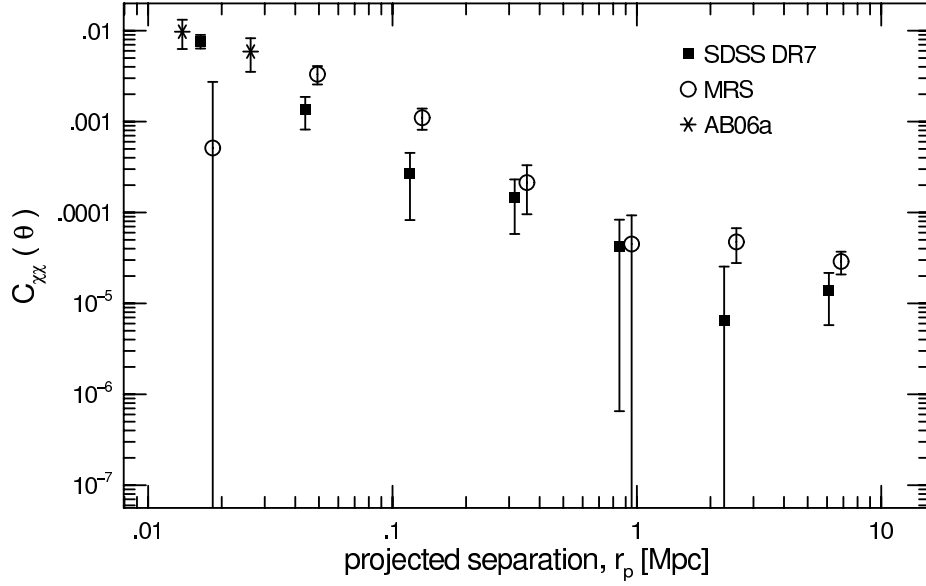


Fig. 4.— Two-point correlation function of galaxy images in the SDSS DR7 (squares) and the Millennium Run Simulation (circles) computed as a function of projected separation on the sky. The data points have been slightly offset in the horizontal direction for clarity. Also shown for comparison (stars) is the small-scale intrinsic alignment found by AB06a for the images of host and satellite galaxies in the SDSS DR4.

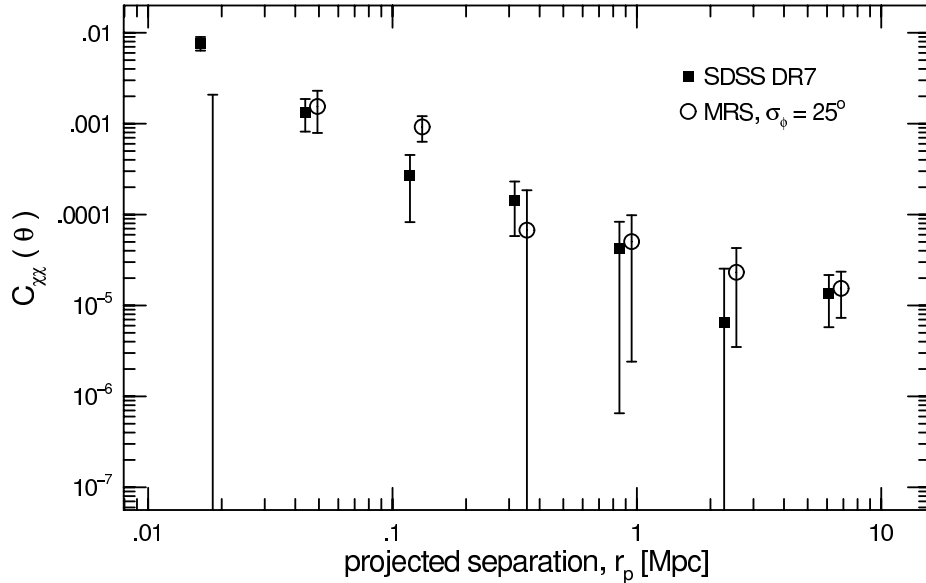


Fig. 5.— Same as Fig. 4, except that Gaussian-random errors with zero mean and dispersion $\sigma_\phi = 25^\circ$ have been added to the position angles of the MRS galaxies. The data points have been slightly offset in the horizontal direction for clarity.

of the galaxies, but it is highly sensitive to errors in the position angles of the galaxies. Therefore, any difference between the intrinsic alignments of theoretical galaxies (e.g., the MRS galaxies in our case) and observed galaxies can, at least in part, be attributed to observational errors associated with position angle measurements. Unfortunately, position angle errors for the SDSS galaxies are not yet available in the archive. Therefore, we cannot place any direct constraints on what fraction of the error needed above is due to observational errors (i.e., determination of the position angles) and what fraction is due to misalignment of mass and light in galaxies. If the contributions are equal (and assuming Gaussian errors), we would require errors of $\sim 17^\circ$ in both cases. Such errors are not unreasonable given what few direct constraints we have on the alignment of mass and light in galaxies, as well as the fact that many SDSS galaxies will have position angles that are challenging to determine (e.g., very round galaxies with smooth light profiles, or disk galaxies that have bright pockets of star formation and/or resolved spiral arms).

4. Dependence of Intrinsic Alignments on Galaxy Properties

Next, we investigate the degree to which the intrinsic alignments of the SDSS and MRS galaxies depend upon various physical properties: $(g - r)$, luminosity, stellar mass, and star formation rate. While each of these properties is known for all of the MRS galaxies, the stellar masses and star formation rates have only been computed for SDSS galaxies that are contained within the DR4. The stellar masses for the SDSS DR4 galaxies were computed by Kauffmann et al. (2003) and the star formation rates were computed by Brinchmann et al. (2004). Our sample of SDSS galaxies with measured stellar masses is therefore reduced to 291,728 and our sample of SDSS galaxies with measured star formation rates is reduced to 297,284.

To divide our sample of galaxies into “red” and “blue” galaxies, we first K-correct the SDSS galaxy colors to the present epoch using the code by Blanton et al. (2003; v4_1_4). We then fit the distributions of $(g - r)$ colors of the SDSS galaxies by the sum of two Gaussians (e.g., Strateva et al. 2001; Weinmann et al. 2006) and we find that the division between the two Gaussians lies at $(g - r) = 0.7$. We therefore define galaxies with $(g - r) < 0.7$ to be “blue” and galaxies with $(g - r) \geq 0.7$ to be “red”. Imposing this criterion, we have 235,834 red galaxies in our sample and 294,563 blue galaxies. To divide our sample of galaxies into a “bright” and “faint” half, we simply use the median r -band absolute magnitude of the SDSS galaxies, $M_r = -21.16$. To divide the sample into a “high stellar mass” and “low stellar mass” sample we use the median stellar mass of the SDSS DR4 galaxies: $\log_{10}(M_*/M_\odot) = 10.61$. Lastly, we define the specific star formation rate (SSFR)

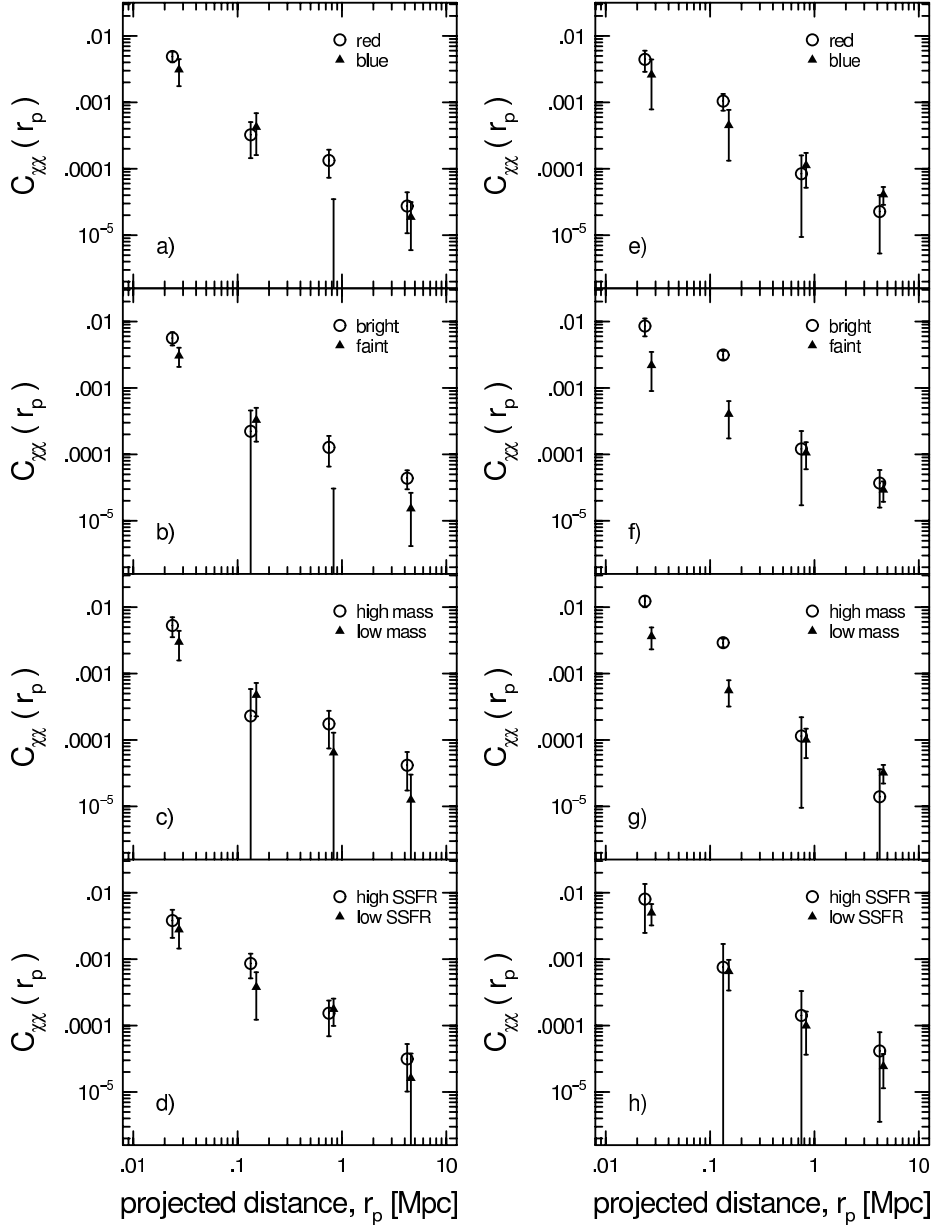


Fig. 6.— Dependence of the two-point image correlation function for SDSS galaxies (left panels) and MRS galaxies (right panels) on a number of physical properties. See text for details regarding the specific subdivisions of the galaxy samples. The data points have been slightly offset in the horizontal direction for clarity.

to be the ratio of the star formation rate (in $M_{\odot} \text{ yr}^{-1}$) to the stellar mass (in solar units), and we divide the sample into a “high SSFR” and “low SSFR” sample using the median SSFR for the SDSS DR4 galaxies: $\log_{10}(\text{SSFR}/\text{yr}^{-1}) = -9.91$.

The results for the dependence of the two–point image correlation function on $(g - r)$, luminosity, stellar mass, and SSFR are shown in Fig. 6. The left panels show the results for the SDSS galaxies, and the right panels show the results for the MRS galaxies. Panels a) and e) show the dependence of $C_{xx}(r_p)$ on $(g - r)$, panels b) and f) show the dependence of $C_{xx}(r_p)$ on luminosity, panels c) and g) show the dependence of $C_{xx}(r_p)$ on stellar mass, and panels d) and h) show the dependence of $C_{xx}(r_p)$ on the specific star formation rate (SSFR). For the most part, the error bars in Fig. 6 for the various subdivisions of the data overlap each other, indicating a rather weak dependence of $C_{xx}(r_p)$ on the properties of the galaxies. To supplement Fig. 6 we therefore compute an average of $C_{xx}(r_p)$ over all values of the projected separation that we have considered, $0.01 \text{ Mpc} \leq r_p \leq 10 \text{ Mpc}$, and we show the results in Table 1.

In the case of the MRS galaxies, the value of $C_{xx}(r_p)$ averaged over $0.01 \text{ Mpc} \leq r_p \leq 10 \text{ Mpc}$ shows essentially no dependence on the properties of the galaxies. That is, for all four subdivisions of the data, the separate values of $\langle C_{xx} \rangle$ agree to within 1σ . In the case of the SDSS galaxies, there is no apparent dependence of $\langle C_{xx} \rangle$ on SSFR. There is a very weak indication (at the 1.4σ and 1.6σ level, respectively) that the red SDSS galaxies are more aligned than are the blue SDSS galaxies, and that the high stellar mass SDSS galaxies are more aligned than are the low stellar mass SDSS galaxies. More convincing is the difference in the intrinsic alignments of the high luminosity SDSS galaxies compared to the low luminosity SDSS galaxies; at the 2.8σ level the high luminosity SDSS galaxies are more strongly aligned on average than are the low luminosity SDSS galaxies. While not definitive, this last result is at least intriguing.

Finally, it is clear from the right hand panels of Fig. 6 that the dependence of $C_{xx}(r_p)$ on projected separation is rather different for the bright and faint MRS galaxies (panel f), as well as for the high and low stellar mass MRS galaxies (panel g). For both the faint and the low stellar mass MRS galaxies, $C_{xx}(r_p)$ appears to be a power law. For both the bright and the high stellar mass MRS galaxies, $C_{xx}(r_p)$ appears to be a broken power law, with a clear change in amplitude at projected radii of order 300 kpc. On scales less than about 300 kpc, $C_{xx}(r_p)$ for the high luminosity MRS galaxies is a factor of order 6 larger than $C_{xx}(r_p)$ for the low luminosity MRS galaxies. Similarly, on scales less than about 300 kpc, $C_{xx}(r_p)$ for the MRS galaxies with high stellar masses is a factor of order 4 larger than $C_{xx}(r_p)$ for MRS galaxies with low stellar masses. It is hard to assess the significance of this, but it may be an indicator that in a redshift survey that is significantly larger than the SDSS, we should

expect to see substantial differences in the intrinsic alignments of high and low luminosity galaxies, as well as high stellar mass and low stellar mass galaxies, at least on scales less than about 300 kpc.

5. Discussion and Conclusions

We have computed the two–point image correlation function for bright galaxies in the SDSS DR7. The function withstands several null tests and, therefore, is more likely to be indicative of intrinsic alignments of the SDSS galaxy images rather than a systematic in the data. On scales greater than $r_p \sim 40$ kpc, the observed two–point image correlation function for the SDSS galaxies has an amplitude that is a factor of order two lower than our prediction for the intrinsic alignment of galaxy images in a Λ CDM universe. The discrepancy between the observed and predicted functions can be eliminated by including a Gaussian–random error on the position angles of the theoretical galaxy images with dispersion $\sigma_\phi = 25^\circ$.

Previous studies of intrinsic alignments of galaxy images have also concluded that the observed alignment of galaxy images is less than predicted. In particular, OJL found that the observed two–point image correlation function for the SDSS LRGs has an amplitude that is a factor of order 4 lower than the predicted function. To explain the discrepancy, OJL claim that mass and light in large elliptical galaxies must be misaligned by $\sigma_\theta = 35.4_{-3.3}^{+4.0}$ degrees. Given the observed alignment of the satellite distribution around large, red SDSS galaxies, as well as observations of weak and strong lensing by early-type galaxies, we expect that such a large misalignment of mass and light in the SDSS LRGs is unlikely. Also, given the fact that the two–point image correlation function is highly sensitive to errors in the measured position angles of the galaxies, at least some of the disagreement between the observed and theoretical functions can be attributed to the finite accuracy with which the position angles of the observed galaxies can be measured. We therefore conclude that, at least in the case of the SDSS galaxies that we have studied, the difference between the observed and predicted two–point image correlation functions can be explained by a combination of modest misalignment of luminous galaxies and their halos, as well as modest position angle errors for the observed galaxy images.

In their study of the intrinsic alignments of galaxy images in the sixth data release of the SDSS, LP07 concluded that for separations greater than $3h^{-1}$ Mpc, the images of red galaxies showed intrinsic alignment, while the images of blue galaxies did not. In our analysis we find at best only weak evidence for a color dependence of the intrinsic alignments, with the red galaxies showing very slightly more intrinsic alignment than the blue galaxies. It is difficult to know why we obtain results that are so different from LP07, but it may have to

do with a combination of the redshifts over which the galaxies were selected as well as the way in which red galaxies were separated from blue galaxies. In LP07, the galaxies were divided into “red” and “blue” samples using $(u - r)$ colors that were not K-corrected. Only 20% of LP07’s galaxies were ultimately classified as being blue, while 56% of our galaxies are classified as being blue. In addition, LP07 used galaxies with redshifts as large as $z = 0.4$, while our sample is restricted to lower redshifts (maximum redshift of $z = 0.2$). Generally, the redder is a galaxy, the more accurate is a measurement of its shape (i.e., since red galaxies tend to have very smooth light profiles). It is also true that, in general, the closer is a galaxy in redshift space (for fixed luminosity), the more accurate is a measurement of its shape. It is, therefore, possible that LP07 were able to measure an intrinsic correlation of the red galaxy images but not the blue galaxy images on scales $r > 3h^{-1}$ Mpc because: [i] the image shapes of the red galaxies were far less noisy than those of the blue galaxies, and [ii] there were simply too few blue galaxies in their sample to detect the intrinsic correlations in the presence of noisy image shapes (i.e., assuming Poisson errors).

In addition to weak evidence for a color dependence of the intrinsic alignments of galaxy images, we also find weak evidence that the degree of intrinsic alignment for the SDSS galaxies is dependent upon the stellar masses (i.e., more massive galaxies show very slightly more alignment than do less massive galaxies). More convincing is the dependence we find on luminosity for the SDSS galaxies; at the $\sim 3\sigma$ level the most luminous SDSS galaxies in our sample show stronger intrinsic alignment than do the least luminous galaxies.

Lastly, we note that we only detect intrinsic alignment of galaxy images when the galaxies are separated by less than 5000 km sec^{-1} along the line of sight. This bodes well for future weak lensing “tomography” experiments that wish to eliminate pairs of galaxy images that may be intrinsically aligned before computing the weak lensing signal. Assuming that the large-scale intrinsic alignments of galaxy images do not persist far beyond $|dv| \sim 5000 \text{ km sec}^{-1}$, this suggests that the use of photometric redshifts with relatively modest accuracy should suffice to eliminate the intrinsic alignment signal from the sought-after weak lensing signal.

Acknowledgments

Support under NSF contract AST-0708468 (TGB, IA, CAM) is gratefully acknowledged. We are also deeply grateful for the public release of the Millennium Run Simulation and its numerous associated databases. Funding for the SDSS and SDSS-II has been provided by the Alfred P. Sloan Foundation, the Participating Institutions, the U.S. Department of Energy, the National Science Foundation, the National Aeronautics and Space Administration,

the NSF, the Japanese Monbukagakusho, the Max Planck Society, and the Higher Education Funding Council for England. The SDSS is managed by the Astrophysical Research Consortium for the Participating Institutions: the American Museum of Natural History, Astrophysical Institute Postdam, University of Basel, University of Cambridge, Case Western University, University of Chicago, Drexel University, Fermilab, the Institute for Advanced Study, the Japan Participation Group, The Johns Hopkins University, the Joint Institute for Nuclear Physics, the Kavli Institute for Particle Astrophysics and Cosmology, the Korean Scientist Group, the Chinese Academy of Sciences (LAMOST), Los Alamos National Laboratory, the Max-Planck-Institute for Astronomy (MPIA), the Max-Planck-Institute for Astrophysics (MPA), New Mexico State University, The Ohio State University, University of Pittsburgh, University of Portsmouth, Princeton University, the U.S. Naval Observatory, and the University of Washington. The SDSS Web site is <http://www.sdss.org>.

REFERENCES

- Abazajian, K. et al. 2009, ApJS in press, astro-ph/0812.0649
- Agustsson, I. & Brainerd, T. G. 2006a, ApJ, 644, L25 (AB06a)
- Agustsson, I. & Brainerd, T. G. 2006b, ApJ, 650, 500
- Agustsson, I. & Brainerd, T. G. 2007, astro-ph/0704.3441
- Aubert, D., Pichon, C. & Colombi, S. 2004, MNRAS, 352, 376
- Azzaro, M., Patiri, S. G., Prada, F., & Zentner, A. R. 2007, MNRAS, 376, L43
- Bailin, J., Power, C., Norberg, P., Zaritsky, D., & Gibson, B. K. 2008, MNRAS, 390, 1133
- Blaizot, J., Wadadekar, Y., Guiderdoni, B., Colombi, S. T., Bertin, E., Bouchet, F. R., Devriendt, J. E. G., & Hatton, S. 2005, MNRAS, 360, 159
- Blandford, R. D., Saust, A.-B., Brainerd, T. G., & Villumsen, J. V. 1991, MNRAS, 251, 600
- Blanton, M. R., Lin H., Lupton, R. H., Maley, F. M., Young, N., Zehavi, I. & Loveday, J. 2003, AJ, 125, 2276
- Brainerd, T. G. 2005, 628, L101
- Bridle, S. & King, L. 2007, New J. Phys., 9, 444
- Brinchmann J., Charlot S., White S. D. M., Tremonti C., Kauffmann G., Heckman T., Brinkmann J., 2004, MNRAS, 351, 1151
- Brown, M. L., Taylor, A. N., Hambly, N. C., & Dye, S. 2003, MNRAS, 333, 501
- Catelan, P., Kamionkowski, M. & Blandford, R. D. 2001, MNRAS, 320, L7
- Crittenden, R., Natarajan, P., Pen, U.-L., & Theuns, T. 2001, ApJ, 559, 552
- Crittenden, R., Natarajan, P., Pen, U.-L., & Theuns, T. 2002, ApJ, 568, 20
- Croft, R. A. C. & Metzler, C. A. 2000, ApJ, 545, 561
- De Lucia, G. & Blaizot, J. 2007 MNRAS, 375, 2
- De Lucia, G., Springel, V., White, S. D. M., Croton, D., & Kauffmann, G. 2006, MNRAS, 366, 499

- Faltenbacher, A., Li, C., White, S. D. M., Jing, Y. P., Mao, S., & Wang, J. 2009, RAA, 9, 41
- Fukugita, M., Ichikawa, T., Gunn, J. E., Doi, M., Shimasaku, K., & Schneider, D. P. 1996, AJ, 111, 1748
- Heavens, A. & Peacock, J. 1998, MNRAS, 232, 339
- Heavens, A., Refregier, A., & Heymans, C. 2000, MNRAS, 319, 649
- Heymans, C., Brown, M., Heavens, A., Meisenheimer, K., Taylor, A., & Wolf, C. 2004 MNRAS, 347, 895
- Heymans, C. & Heavens, A. 2003, MNRAS, 339, 711
- Heymans, C., White, M., Heavens, A., Vale, C., & van Waerbeke, L. 2006, MNRAS, 371, 750
- Hirata, C. M. & Seljak, U. 2004, Phys. Rev. D, 70, 63526
- Hoekstra, H., Yee, H. K. C., & Gladders, M. D. 2004, ApJ, 606, 67
- Hogg, D. W., Finkbeiner, D. P., Schlegel, D. J., & Gunn, J. E. 2001, AJ, 122, 2129
- Ivezić, Z. et al. 2004, Astronomische Nachrichten, 325, 583
- Joachimi, B. & Schneider, P. 2008, AA, 488, 829
- Jing, Y. P. 2002, MNRAS, 335, L89
- Kauffmann G., Heckman, T. M., White, S. D. M., Charlot, S., Tremonti, C., Peng, E. W., Seibert, M., Brinchmann, J., Nichol, R. C., SubbaRao, M., & York, D. 2003, MNRAS, 341, 33
- Keeton, C. R., Kochanek, C. S. & Falco, E. E. 1998, ApJ, 509, 561
- King, L. & Schneider, P. 2003, AA, 398, 23
- Kitching, T. D., Amara, A., Abdalla, B., Joachimi, B., & Refregier, A. 2008, astro-ph/0812.1966
- Lee, J. & Pen, U.-L. 2001, ApJ, 555, 106
- Lee, J. & Pen, U.-L. 2007, ApJ, 670, L1 (LP07)

- Lee, J., Springel, V., Pen, U.-L., & Lemson, G. 2008, MNRAS, 389, 1266
- Mackey, J., White, M. & Kamionkowski 2002, MNRAS, 332, 788
- Mandelbaum, R. Seljak, U., Kaffmann, G., Hirata, C. M., & Brinkmann, J. 2006, MNRAS, 370, 1008
- Okumura, T., Jing, Y. P., & Li, C. 2009, ApJ, 694, 214 (OJL)
- Parker, L., Hoekstra, H., Hudson, M., van Waerbeke, L., & Mellier, Y. 2007, ApJ, 669, 21
- Porciani, C., Dekel, A. & Hoffman, Y. 2002, MNRAS, 332, 325
- Schneider, M. D. & Bridle, S. 2009, astro-ph/0903.3870
- Siverd, R. J., Ryden, B. S. & Gaudi, B. S. 2009, ApJ submitted, astro-ph/0903.2264
- Smith, J. A. et al. 2002, AJ, 123, 2121
- Springel, V., et al. 2005, Nature, 435, 629
- Strateva I., et al., 2001, ApJ, 122, 1861
- Strauss, M.A. et al. 2002, AJ, 124, 1810
- Takada, M. & White, M. 2004, ApJ, 601, L1
- Weinmann, S. M., van den Bosch, F. C., Yang, X., & Mo, H. J., 2006, MNRAS, 366, 2
- York D. G., et al. 2000, AJ, 120, 1579
- Zhang, P. 2008, astro-ph/0811.0704

Table 1: $C_{\chi\chi}(r_p)$ averaged over $0.01 \text{ Mpc} \leq r_p \leq 10 \text{ Mpc}$

	SDSS galaxies	MRS galaxies
Red	$(3.74 \pm 1.61) \times 10^{-5}$	$(2.97 \pm 1.69) \times 10^{-5}$
Blue	$(1.80 \pm 1.25) \times 10^{-5}$	$(4.44 \pm 1.20) \times 10^{-5}$
Bright	$(4.88 \pm 1.35) \times 10^{-5}$	$(4.64 \pm 2.07) \times 10^{-5}$
Faint	$(1.50 \pm 1.07) \times 10^{-5}$	$(3.34 \pm 0.97) \times 10^{-5}$
High M_*	$(5.03 \pm 2.35) \times 10^{-5}$	$(2.62 \pm 2.18) \times 10^{-5}$
Low M_*	$(1.93 \pm 1.69) \times 10^{-5}$	$(3.61 \pm 0.98) \times 10^{-5}$
High SSFR	$(4.36 \pm 2.06) \times 10^{-5}$	$(4.68 \pm 3.71) \times 10^{-5}$
Low SSFR	$(3.11 \pm 2.09) \times 10^{-5}$	$(2.86 \pm 1.26) \times 10^{-5}$